

Dixon Imaging of Bone stress injury of knee- comparison to conventional Intermediate-weighted MR imaging

Avneesh Chhabra^{1*}, Parham Pezeshk¹, Riham Dessouky^{1,3}, Orlando Morales¹ and Jay Shah²

¹Radiology, University of Texas Southwestern Medical Center, Dallas, TX, USA

²Orthopaedic Surgery, University of Texas Southwestern Medical Center, Dallas, TX, USA

³Radiology, Faculty of Medicine, Zagazig University, Zagazig, Egypt

Abstract

Objectives: Dixon sequence is a chemical shift-based MR sequence that produces four sets of images (water only, fat only, in-phase, and out-of-phase) images and is currently being used in various musculoskeletal applications. The aim of this study was to test the sensitivity of detection and determine the extent of the lesion on the Dixon imaging versus conventional proton density weighted (PDW) imaging in the domain of bone stress injury (BSI) and obtain inter-reader performance.

Methods: In this retrospective cross-sectional study, 32 consecutive BSI were compared on conventional imaging versus different Dixon images in terms of area of bone marrow edema, inter-trabecular fracture detection and fracture conspicuity. Inter-reader reliability was also evaluated. $p < 0.05$ was considered statistically significant.

Results: The Dixon imaging showed excellent quality except two cases with some motion degradation. BSI detection on Dixon water image is equivalent to the routine fat suppressed fluid sensitive intermediate weighted sequence. BSI area on water image is not significantly different from the intertrabecular lesion area on opposed-phase imaging ($p = 0.9531$). The opposed-phase images detected more number of fractures than the water, PDW, & in-phase images ($p < 0.0001$, $= 0.0008$, and < 0.0001 , respectively) with superior fracture conspicuity than the water, PDW, & in-phase images (p value < 0.0001 , $= 0.0085$, and $= 0.0035$, respectively). Fair to moderate inter-reader agreement was seen.

Conclusions: Dixon imaging is as sensitive as conventional fat suppressed fluid sensitive imaging of the knee for the identification of bone bruise with superior detection and improved characterization of the intertrabecular fractures.

Advances in knowledge: In the domain of bone stress injury (BSI), Dixon opposed-phase MR images detect more number of fractures with better conspicuity than water-only, PDW, and in-phase images.

Keywords: Chemical shift imaging, Dixon Imaging, Bone stress injury, Bone bruise, MRI.

Introduction

Bone stress injuries are common in various sports. Basketball injuries are among the most common of all sports injuries (representing 23.1% of all sports injuries) [1-3] with an injury rate of 18.3 per 1000 participants and no significant gender and anthropomorphic differences [4]. Serious injuries including bone stress injuries (BSI) are seen at a rate of 2.89/1,000 participations and the most common sites of involvement are observed in the lower extremity, i.e., the ankle joint, the calf/anterior leg, and knee joint [5]. MRI is the modality of choice to detect occult BSI, and to evaluate associated internal joint derangements and regional muscles [6,7]. Bone bruise is identified as edema signal on fluid sensitive fat suppressed imaging on MRI as early as 1 hour after the injury [8]. Bone bruises are associated with pain and are shown to resolve in 3-9 months' time following the injury [9]. Persistent bone bruise, overlying cartilage injury and higher MRI grade of BSI have been shown to predispose to delayed return-to-play [10-12]. It is not clear why bone bruises persist longer in some patients and it may be hypothesized that such non-resolving or slowly resolving lesions may encompass underlying inter-trabecular fracture or excessive hemorrhage that would

prolong their resolution. Regular orthopedic sports MRI protocols commonly include intermediate weighted nonfat-suppressed and fat-suppressed proton density (PDW) imaging sequences [7,13]. In a small series, opposed phase T1W chemical shift imaging (CSI) was shown to detect more inter-trabecular abnormality than the conventional T1W imaging [14] However, it is often difficult to differentiate edema from fracture on T1W CSI due to similar signal intensity alteration. Intermediate-weighted Dixon imaging provides better fluid sensitive contrast than T2W CSI and generates multiple images, i.e., in-phase, opposed-phase, water and fat [15-19]. This study was intended to test the sensitivity of detection and determine the extent of the lesion on Dixon imaging versus conventional PDW imaging in the domain of bone stress injury (BSI) and obtain inter-reader performance. The hypothesis was that opposed-phase imaging is better at detecting intertrabecular abnormality and fractures as compared to the conventional PDW sequence with good inter-observer agreement..

Methods

This was a retrospective institutional review board approved cross-sectional study performed with HIPAA compliance and informed consent was waived. .

Patient selection

Our county hospital picture archiving and communication system was queried for consecutive knee MRIs, age range 18-50 years, and the following words- 'bone stress injury', 'bone contusion', 'inter-trabecular fracture', and 'bone bruise' over a period of 7 months (9/2015-3/2016). 25 MRIs were found to include Dixon imaging and above injuries. Seven MRI scans were excluded due to reasons, such as an obvious displaced fracture, insufficiency injury with underlying osteopenia, articular cartilage loss related subchondral reactive bone marrow edema, ankle fracture, and prior surgery related changes. Since some knees contained multiple bone stress injuries (BSIs), all injuries above 10-millimeter (mm) bruise area (edema signal on fat suppressed PDW or short tau inversion recovery, STIR) were included.

MR imaging

All imaging studies was performed on 1.5 Tesla (T) or 3T scanners. The imaging was obtained using a dedicated knee coil in the supine position. The general protocol parameters are outlined in Table 1. Regardless of the scanner, the Dixon was obtained in the axial plane with same parameters of repetition time, echo time, and matrix.

Data collection

The patient demographics (age, gender, laterality, history of fall/motor vehicle accident) were recorded. The MRI scanner strength and dates were noted. The available radiographs within four weeks of MRI were evaluated for presence or absence of abnormality related to stress injury (0- neg, 1- positive for fracture, 2 –focal lucency, 3- avulsed frag). The MRI reports from electronic health records were accessed. Qualitative assessment of the Dixon images was performed by reader 1 using a semiquantitative 4-point Likert scale to grade the artifacts due to image distortion, water fat swap artifacts, and motion: 1, none; 2, low; 3, moderate; 4, high. The reader also confirmed and recorded the previously reported presence of associated meniscus tears, cruciate or collateral ligament injuries.

Image reading procedures

Two musculoskeletal fellowship trained readers (radiologists with 9 years [reader 1] and 3 years [reader 2] of teaching level attending experience) independently evaluated all images following a consensus reading of 3 studies and 4 different BSI on picture archiving and communication system (PACS). The following pulse sequences were evaluated, and data recorded for individual BSIs on all studies-

- a Fat suppressed sagittal and coronal PDW / STIR images (routine fluid-sensitive imaging) - to confirm a bone stress

injury-bone marrow edema absent (0) or present (1).

- b Corresponding sagittal and coronal nonfat-suppressed PDW images (routine imaging) - fracture line as linear or fluid like focal hypointensity, absent (0) or present (1). If present, the fracture conspicuity was graded as: 1-extremely sharp, 2-moderately sharp and mostly continuous, 3-somewhat sharp and broken, 4- minimal and ill-defined.
- c Axial Dixon water image- bone marrow edema absent (0) or present (1). Area of edema in mm2. Fracture line, absent (0) or present (1). If present, the fracture conspicuity was graded as: 1-extremely sharp, 2- moderately sharp and mostly continuous, 3-somewhat sharp and broken, 4- minimal and ill-defined.
- d Axial Dixon in-phase image- area of lesion in mm2. Fracture line, absent (0) or present (1). If present, the fracture conspicuity was graded as: 1-extremely sharp, 2-moderately sharp and mostly continuous, 3-somewhat sharp and broken, 4- minimal and ill-defined.
- e Axial Dixon opposed-phase image- area of inter-trabecular abnormality in mm2. Fracture lines, absent (0) or present (1). If present, the fracture conspicuity was graded as: 1-extremely sharp, 2- moderately sharp and mostly continuous, 3-somewhat sharp and broken, 4- minimal and ill-defined.
- f Percentage loss of signal on opposed phase vs in-phase- it was calculated in both area of concern as well as corresponding normal appearing opposite femoral or tibial condyle without bone marrow edema.

Statistical procedures

All data were recorded on Microsoft excel (2010) and were analyzed using SAS 9.4 software (SAS Institute Inc., Cary, NC, USA). The results were summarized as means \pm SD and medians. Box plots and bar charts were generated to illustrate the measured edema area and number of fractures detected on each modality. The abnormal bone marrow area on opposed phase imaging were compared to those from in-phase and Dixon water images using linear mixed model with Dunnett adjustment for multiple comparisons. Generalized estimating equation was used to test the Dixon images effect in detecting fractures and fracture conspicuity. For inter-reader agreements, Bland-Altman plots, Intraclass correlations (ICC), %agreements, and kappa statistics were performed for continuous and categorical variables, respectively. Paired t-test was used to test the difference in percent loss of signal on opposed phase vs in-phase images between BSI and normal regional bone marrow. P-value<0.05 was considered statistically significant.

Sequence	Repetition time	Echo time	Acquisition Time	Matrix	Slice thickness (mm)
Coronal 3D TSE	1200	38	6:52	320x320	Voxel: 0.6x0.6x0.6
Coronal PDW	3770	40	4:20	384x384	3
Coronal fat suppressed PDW	3900	35	4:30	384x384	3
Sagittal PDW	3110	31	3:30	320x288	3
Sagittal fat suppressed PDW	3570	31	3:40	320x288	3
Axial Dixon	6030	59	4:40	320x256	3

Table. 1: MRI Knee protocol on 3T scanner.

Number and gender of patients	11 men	7 women
Number of BSI	21/32 men	11/32 women
History	12/18- sports injury &/or fall	3/18- MVA
Radiographs	6/18- positive	12/18- negative
Age	35+/-13 (mean +/-SD)	32 (median)
Location of BSI	16/32- tibia	16/32- femur
Knee laterality	19/32- right knee	13/32- left knee
Scanner strength	4/18- 1.5T	14/18- 3T
Meniscus tears	6/18- medial meniscus	5/18- lateral meniscus
Cruciate ligament tears	8/18- anterior cruciate	5/18- posterior cruciate
Collateral ligament tears	5/18- medial collateral	4/18- lateral collateral

Table 2. Descriptive statistics of demographics, radiographs and MRI findings.



Figure 1. 18-year-old female with soccer injury related BSI. Coronal routine fat suppressed A) and B) nonfat-suppressed PDW images show bone marrow edema of the proximal lateral tibia. Axial T2 Dixon images show similar edema (c- small arrow on water image), no abnormality on the in-phase image (d- medium arrow) and a conspicuous intertrabecular fracture on opposed-phase image (e- large arrow).

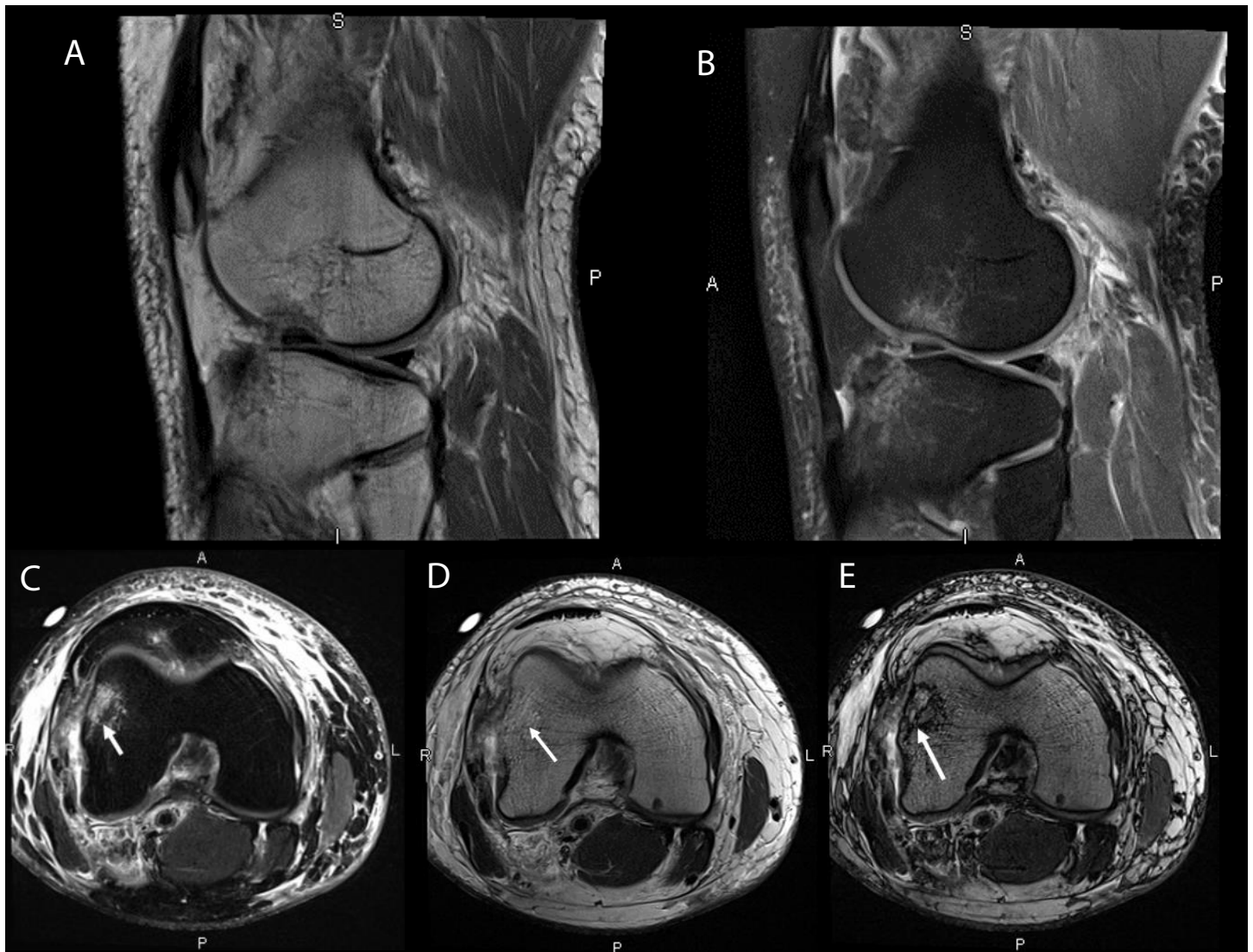


Figure 1. 24-year-old man with MVA. The displaced anterior tibial plateau fracture seen on sagittal PDW and fat suppressed PDW images. A,B) was excluded from the analysis. The lateral femoral condyle BSI was graded as, C) water image (area- 21x10mm, fracture-0, small arrow), (a) PDW image (fracture-1, conspicuity-2), D) in-phase image (area- 19x12mm, fracture-0, medium arrow), E) opposed phase image (area- 21x11mm, fracture-1, conspicuity-2, large arrow).

	Number of fractures	
	Reader 1	Reader 2
IP	8	10
OP	29	31
PD	21	22
fat sat	8	9

Table 2. Number of fractures detected by the two readers on different images of Dixon sequence.

Dixon MR sequence Maps	Area of fracture (ICC)	Fracture detection (kappa)		Fracture conspicuity (weighted kappa)	
		% agree	Kappa	% agree	Kappa
Water	0.989139	83.33333	0.590164	100	1
Opposed phase	0.915549	93.75	0.47541	58.62069	0.358908
In-phase	0.931399	93.75	0.846154	50	0.130435
PDW		96.875	0.929204	61.90476	0.624255

Table 4. Inter-reader agreement in evaluation of BSI on Dixon imaging.

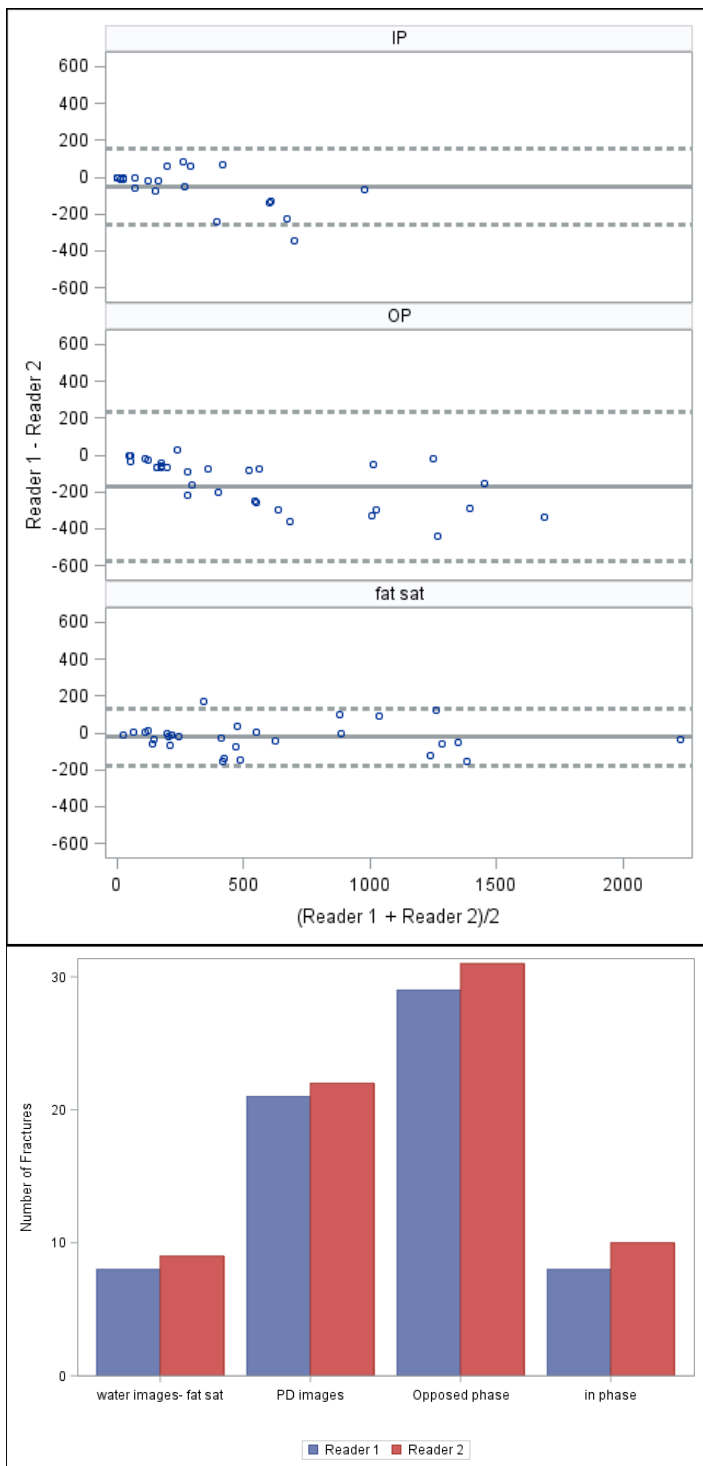


Figure 3. A) The bland Altman plots using different images of the Dixon sequence show the agreement in fracture area measurements between readers. B) The bar chart shows that opposed-phase images detected the most number of fractures.

Results

There were 32 BSI appearing as edema like signal on the routine fluid sensitive imaging in 18 patients (11 men and 7 women with ages 35 ± 13 , 32 [mean \pm SD, median]. Two studies were degraded by moderate degree of motion artifacts, one by low degree, and the remaining were of excellent quality. Table 2 outlines the descriptive statistics of demographics, scanner strength, radiographic findings,

location of BSI, and associated soft tissue injuries.

The bone marrow edema signal was similarly observed on the Dixon water images in all cases and no cases of BSI were missed. The mean area on Dixon water images was (543 ± 526 mm²), which was not significantly larger than the intertrabecular abnormality on opposed phase imaging (483 ± 437 , $p=0.9531$) and was significantly higher than that of in phase images ($p<0.0001$) (Figure 1 and Figure 2). The bland Altman plots using different images of the Dixon sequence showed that agreement in fracture area measurements were better when the areas were small and became worse when areas were larger.

Significantly more fractures were detected on opposed-phase images than the in-phase ($p<0.0001$), proton density images ($p=0.0008$) and water images ($p<0.0001$). The opposed-phase images detected 21 more fractures than the water images (29 vs. 8 and $P<0.0001$ [McNemar test]), conventional PDW (29 vs. 21 and $p=0.0008$), and in-phase images (29 vs. 8 and $p<0.0001$) (Table 3). The fracture conspicuity score (lower the better) on the opposed-phase images was lower than the water ($p<0.0001$), proton density (p value= 0.0085), and in-phase images (p value= 0.0035). The inter-reader agreement is shown in Fig. 3 and Table 4.

The inter-reader agreement in calculation of the area of fracture was excellent ($ICC=0.92-0.99$) on different Dixon images. The % agreement in fracture detection was 83-97% among different images. There was fair to moderate agreement on the opposed-phase images regarding the fracture detection and conspicuity, the sequence which showed the most number of fractures ($kappa=0.48$ and 0.35 , respectively).

The mean % loss of signal at the site of BSI on opposed phase vs in-phase images was $67\% \pm 11\%$, which was significantly more loss than normal regional bone marrow ($32\% \pm 6\%$, $p<0.0001$).

Discussion and conclusion

The findings validate the use of T2 Dixon imaging in the domain of bone stress injury (BSI) around the knee with no cases of BSI missed as compared to the current reference standard, PDW and fat suppressed PDW MR imaging sequences. The image quality was excellent in most cases. With good fluid contrast on intermediate weighted Dixon imaging, the inter-trabecular fractures were easily identified as reflected in the superior conspicuity scores and more fractures observed on the opposed phase imaging. The inter-reader agreement was fair to moderate. Kappa probably underestimated the true agreement due to imbalanced (skewed) sample. As a result, we also presented percentage agreement as a surrogate. There was significant loss of signal on opposed imaging as compared to the in-phase imaging on intermediate weighted Dixon imaging, as has also been reported in the previous studies using T1W CSI for benign versus malignant lesions and benign versus malignant fractures [20]. Dixon-based fat quantification MRI has been extensively used in evaluation of hepatic steatosis, as well as recently in the assessment of intra-muscular steatosis such as in hip abductor and paraspinal skeletal muscle groups [15-18]. To our knowledge, BSI has not been studied before using Dixon imaging.

The BSI has been traditionally graded on a scale of I-IV in an original article by Fredericson et al. [21]. For the prediction of return-to-play, Nattiv et al. [10] further modified the grading system and correlated with the clinical outcomes. It is still not clear as to which bone bruises persist longer or impact the patient prognosis adversely. Dixon imaging allows calculation of the area of intertrabecular abnormality as well as fractures. Water images afford assessment of the co-existent soft tissue injuries. Thus, it is a useful sequence with multiple tissue contrasts.

The intent of this study was validation of the Dixon imaging in the domain of BSI. We did not correlate with CT imaging as BSI

marrow lesions are often occult on CT, or the clinical findings of follow-up or return-to-play due to the incomplete follow-up electronic health records in this retrospective evaluation. The readers evaluated all images together as they could not be blinded to different tissue contrasts on PACS, however every effort was made to objectively assess the lesions on different sequences.

The clinical response of these injuries is judged by validated measures, such as VAS (visual analogue scale for pain), IKDC (international knee documentation committee) and Marx activity scale. In future, a prospective study can be performed to determine the patient outcomes using surrogate imaging markers, such as the using bone bruise area, inter-trabecular fracture area, and associated meniscus, cruciate or collateral ligament injuries. Simultaneously studying multiple image parameters of BSI has the potential to generate markers for determination of prognosis and would represent a significant advance in the care of BSI. The results may help researchers better understand the BSI in the clinical setting and generate determinants for outlining the treatment strategies and predicting patient prognosis.

In conclusion, Dixon imaging is as sensitive as conventional fat suppressed fluid sensitive imaging of the knee for the identification of bone bruise with superior detection and improved characterization of the intertrabecular fractures.

References

1. Powell JW, Barber-Foss KD. Sex-related injury patterns among selected high school sports. *Am J Sport Med.* 2000; 28: 385-391.
2. Emery CA, Meeuwisse WH, McAllister JR. Survey of sport participation and sport injury in Calgary and area high schools. *Clin J Sport Med.* 2006; 16: 20-26.
3. Burt CW, Overpeck MD. Emergency visits for sports-related injuries. *Ann Emerg Med.* 2001; 37: 301-308.
4. McKay GD, Goldie PA, Payne WR, Watson LF. A prospective study of injuries in basketball: A total profile and comparison by gender and standard of competition. *J Sci Med Sport.* 2001; 4: 196-211.
5. Iwamoto J. Analysis of stress fractures in athletes based on our clinical experience. *World J Orthop* 2011;2:7.
6. Major NM, Helms CA. MR imaging of the knee: Findings in asymptomatic collegiate basketball players. *Am J Roentgenol.* 2002; 179: 641-644.
7. Kaplan LD, Schurhoff MR, Selesnick H, Thorpe M, Uribe JW. Magnetic resonance imaging of the knee in asymptomatic professional basketball players. *Arthroscopy.* 2005; 21: 557-561.
8. Blankenbaker DG, De Smet AA, Vanderby R, McCabe RP, Koplin SA. MRI of acute bone bruises: timing of the appearance of findings in a swine model. *Am J Roentgenol.* 2008; 190: W1-W7.
9. Davies NH, Niall D, King LJ, Lavelle J, Healy JC. Magnetic resonance imaging of bone bruising in the acutely injured knee--short-term outcome. *Clin Radiol.* 2004; 59: 439-445.
10. Nattiv A, Kennedy G, Barrack MT, Abdelkerim A, Goolsby MA, et al. Correlation of MRI grading of bone stress injuries with clinical risk factors and return to play: A 5-year prospective study in collegiate track and field athletes. *Am J Sports Med.* 2013; 41: 1930-1941.
11. Boks SS, Vroegindewij D, Koes BW, Hunink MGM, Bierma-Zeinstra SAM, et al. Follow-up of Occult Bone Lesions Detected at MR Imaging: Systematic Review. *Radiol.* 2006; 238: 853-862.
12. Filardo G, Kon E, Tentoni F, Andriolo L, Martino AD, et al. Anterior cruciate ligament injury: post-traumatic bone marrow oedema correlates with long-term prognosis. *Int Orthop.* 2016; 40: 183-190.
13. Wadhwa V, Malhotra V, Xi Y, Nordeck S, Coyner K, et al. Bone and joint modeling from 3D knee MRI: Feasibility and comparison with radiographs and 2D MRI. *Clin Imaging.* 2016; 40: 765-768.
14. Zampa V, Carafoli D, Grassi L, Cosottini M, Trippi D, et al. Usefulness of opposed-phase gradient-echo technique in the diagnosis of occult lesions of the knee and comparison with traditional T1-weight sequences (in-phase). *Radiol Med.* 2000; 99: 31-35.
15. Marcon M, Berger N, Manoliu A, Fischer MA, Nanz D, et al. BN. Normative values for volume and fat content of the hip abductor muscles and their dependence on side, age and gender in a healthy population. *Skelet Radiol.* 2016; 45: 465-474.
16. Mhuiris AN, Volken T, Elliott JM, Hoggarth M, Samartzis D, et al. Reliability of quantifying the spatial distribution of fatty infiltration in lumbar paravertebral muscles using a new segmentation method for T1-weighted MRI. *BMC Musculoskelet Disord.* 2016; 17: 234.
17. Agten CA, Roskopf AB, Gerber C, Pfirrmann CWA. Quantification of early fatty infiltration of the rotator cuff muscles: comparison of multi-echo Dixon with single-voxel MR spectroscopy. *Eur Radiol.* 2016; 26: 3719-3727.
18. Lee S, Lucas RM, Lansdown DA, Nardo L, Lai A, et al. Magnetic resonance rotator cuff fat fraction and its relationship with tendon tear severity and subject characteristics. *J Shoulder Elb Surg.* 2015; 24: 1442-1451.
19. Pezeshk P, Alian A, Chhabra A. Role of chemical shift and Dixon based techniques in musculoskeletal MR imaging. *Eur J Radiol.* 2017; 94: 93-100.
20. Zajick DC, Morrison WB, Schweitzer ME, Parellada JA, Carrino JA. Benign and Malignant Processes: Normal Values and Differentiation with Chemical Shift MR Imaging in Vertebral Marrow. *Radiol.* 2005; 237: 590-596.
21. Fredericson M, Bergman AG, Hoffman KL, Dillingham MS. Tibial Stress Reaction in Runners: Correlation of Clinical Symptoms and Scintigraphy with a New Magnetic Resonance Imaging Grading System. *Am J Sports Med.* 1995; 23: 472-481.

***Correspondence:** Avneesh Chhabra, Radiology, University of Texas Southwestern Medical Center, Dallas, TX, USA, Tel: (+1) 2146482122; Email: avneesh.chhabra@utsouthwestern.edu

Rec: 01 Sep 2020; **Acc:** 25 Sep 2020; **Pub:** 28 Sep 2020

J Clin Med Imag. 2020;3(2):125
DOI: 10.36879/JCMI.20.000125

Copyright © 2020 The Author(s). This is an open-access article distributed under the terms of the Creative Commons Attribution 4.0 International License (CCBY).